Mechanical Analysis of Human DBS Electrodes

H.H Draz
Department of Microelectronics
Electronics Research Institute
Giza Egypt 12622
Email: hdraz@eri.sci.eg

Eslam Elmitwalli
and Mirna Soliman
Nanotechnology Department
Zewail City of Science
and Technology

S.R.I Gabran
Department of Electrical
and Computer Engineering
CIRFE Lab
University of Waterloo
Waterloo Canda

Mohamed Basha
Department of Electrical
and Computer Engineering
CIARS
University of Waterloo
Waterloo Canda

Hassan Mostafa
Electronics and
Communications Department
Faculty of Engineering
Cairo University
Giza Egypt 12316
Email: hmostafa@uwaterloo.ca

Mohamed Abu-Elyazeed
Electronics and
Communications Department
Faculty of Engineering
Cairo University
Giza Egypt 12316

Amal Zaki
Department of Microelectronics
Electronics Research Institute
Giza Egypt 12622

***Abstract*—Deep brain stimulation (DBS) electrodes have been proved to be effective in treating neural related diseases in rodents. These devices were successfully extended to the field of human neuro therapy. Many different electrodes exist. However, no quantitative ranking criterion is available to allow meaningful comparison of the various DBS electrodes to aid the designer.**

This paper presents a novel Figure of Merit (FOM) dedicated to DBS electrodes. The proposed optimization performance takes into account safety factors of mechanical analysis and the estimated fabrication cost of some materials. The FOM is used to rank several DBS electrode designs.

Finite Element Models (FEM) analysis for several electrode layouts are conducted. FEM shows the effects of different design parameters on the electrode mechanical performance. These parameters include electrode dimensions, geometry, and materials. The electrodes mechanical analysis is evaluated from different points of view including: linear buckling analysis, stationary analysis with axial and shear loading. The safety factors are calculated for several designs with different materials (brittle and ductile materials). The results obtained from FEM mechanical analysis for the various electrodes prototypes are presented, which provide guidelines for different electrode designs and material choice. A proposed fabrication process along with an estimated fabrication cost is also introduced.

Keywords*—*Stimulation Electrode, FEM, Buckling Analysis, Stationary Analysis, Figure of Merit, Fabrication Cost.

I. Introduction

Human brain is a very envolved networked-structure made up of billions of nerve cells, known as neurons. This brain could lose part of its functionality when many cells are lost as a result of developmental effects, strokes or tumor amputation. For example, these disorders can lead to deficiency in the motor system, which is known as Parkinson disease. It could also produce abnormal signals from the brain, causing bizarre sensations, behaviors, emotions and sometimes loss of consciousness. Such disease is known as Epilepsy.

Recently, deep brain stimulation (DBS) microelectrodes proved their efficiency in the therapy of neural disorders, where the electrodes are implanted in the malfunctional brain region, and by sending electrical signals, these disorders are resolved. So far, many developments have been introduced to deep brain stimulation electrodes, starting with glass micropipettes and followed by microwire bundle electrodes [1], [2].

With the emergence of micromachined micro-fabrication techniques, micromachined electrodes were capable of overcoming the limitations introduced by the microwire electrodes [3]. And finally reaching the latest implementable technique; flexible electrodes, which are compatible with the brain tissues [1].

The electrode structural designs, dimensions and the materials are used to portray the essential factors that mainly affect the electrode performance. Regarding the electrode size, it must be as small as possible in order to avoid damaging many surrounding neural cells. As for the electrode structure, it must be rigid enough to ensure successful insertion, yet at the same time, it must be flexible and biocompatible to suit the brain environment.

Recently, some types of deep brain stimulation electrode have appeared such as foldable neural electrode [4]. This microfabricated electrode is a type of flexible DBS electrode of the cavity wall of thalamic lesions resulting from brain infarcts. It is allowing stimulation at different anatomical locations. It is fabricated from Polyimide and its length is 40 mm so it needs an insertion assistive device through penetration surgery and on implantation, the electrode is introduced through a cannula. Another type is an implantable micromachined neural probe with multichannel electrode for both recording and electrical stimulation was designed [5]. This flexible, Polyimide-based microelectrode is composed of a long shaft (14.9 mm in length) with small thickness $5\,\mu\mathrm{m}$. So this electrode with this dimensions will need an insertion assistive device during implementation. The human DBS electrodes have a variable

range of the shaft length from 6mm to 40mm in some papers.

In this paper, several electrode layout designs with different materials are introduced and their mechanical analysis during insertion into the brain tissues is studied. From this analysis, a prediction of which design, with which material and which dimensions will overcome the mechanical failure and can be implemented without needing an insertion assistive device. Electrode mechanical analysis is presented with two mechanical failure modes the electrode is subjected to on insertion: buckling and fracture. Thus, linear buckling analysis and stationary analysis with axial and shear loading are illustrated for both brittle and ductile materials with the help of COMSOL Multiphysics. These electrode layouts are juxtaposed to estimate which design achieves the best critical load and safety factor due to the applied forces.

Finally, a FOM is calculated for each design, which is considered as a numerical quantity based on one or more characteristics of the design to represent a measure of efficiency. Low impedance, low noise, low fabrication cost, small cross section area, large number of channels, and high safety factor of mechanical analysis are the characteristics of FOM. In this work, the comparative analysis is between the designs with different fabrication cost and safety factors, and the other characteristics are constant for all designs [6].

This paper is organized as follows: Methods Section explains the different mechanical designs, presents finite element models for several electrode layouts, and also shows the mechanical forces which affect the electrode failures influencing it. Fabrication Section illustrates the fabrication process and its cost. Results Section exposes electrode mechanical performance with various analysis techniques including: linear buckling analysis, stationary (static) analysis with axial and shear loading, and failure analysis for brittle and ductile materials and a comparison among all designs with a focus on FOM results. Finally the conclusion is drawn in the last Section.

II. Electrode Mechanical Designs and Analysis

A. Electrode Mechanical Designs

Several designs were proposed based on initial designs for rat electrodes [7]. All the design are illustrated in Figure 1. The shaft length was increased to 10mm to be suitable for the human brain [8]. In order to compare the different designs, the thickness was made constant at $100\,\mu\mathrm{m}$ for all electrodes. The minimum width for the shaft was also equal for all designs at $130\,\mu\mathrm{m}$. The initial designs mostly differed in base design and dimensions.

The electrodes had different base designs except for design A and B. Both designs are similar except for the shaft. Design B has a shaft with two stages descending in width and length. The first stage of the shaft which is the nearest part to the base is the widest stage and is nearly two thirds of the total length. The wider shaft increases total area but on the other hand, the mechanical properties, specifically buckling resistance is expected to improve. The idea to divide the shaft into several stages was expanded up to 5 stages for design B as can be seen in Figure 2.

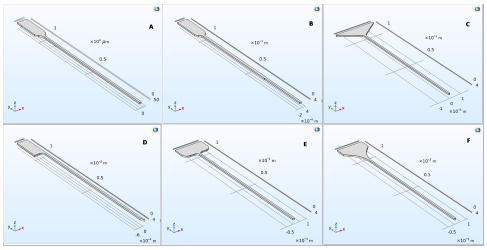

Fig. 1. Several designs of human electrodes based on initial designs for rat electrodes.

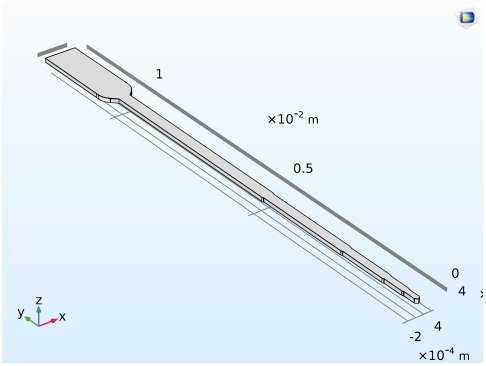

Fig. 2. Design B with five stages, each stage wider than the following stage by $40\,\mu\mathrm{m}$ and is double its length.

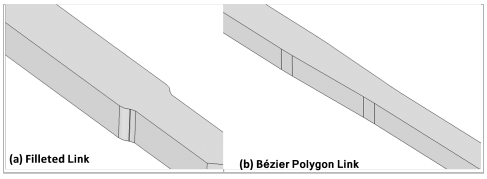

Fig. 3. 2 different ways to make smoothing shaft, (**a**) The model with high stress on the edges of the stages because its sharp shape. (**b**) The model with high stress on the edges of the stages because of its smoothing shape.

The staged design is also applied to designs C, D, E and F. A comparative analysis between the different designs up to three stages was carried out with shaft width of different stages ranging from $210\,\mu\mathrm{m}$ to $130\,\mu\mathrm{m}$. All designs followed the same shaft design to allow for a proper comparison between the different bases.

The region connecting the different stages is expected to develop high stress due to the abrupt change in width. Accordingly, sharp edges, which are illustrated in Figure 3:a are filleted to allow for a smoother transition.

Another method that allowed for a smoother transition is developed using Bzier Polygons [9], as in Figure 3:b, to alleviate stress from the intermediate regions.

It is important to note that the device total area should be kept minimum as long as we dont sacrifice its mechanical integrity. Although the staged design increases shaft area, it is intended to reconcile with better mechanical performance. Different design ideas are also applied to the staged design for the sake of providing a comparative insight between varying stage lengths. Three different ideas are further explored in this paper; equal stage lengths is illustrated in Figure 4a , longest first stage is illustrated in Figure 4b and longest final stage is

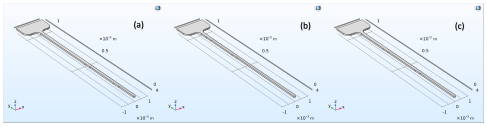

Fig. 4. 3 different designs of the shafts, (**a**) The modeled shaft with Longest first stage. (**b**) The shaft with longest last stage. (**c**) The shaft with equal stages.

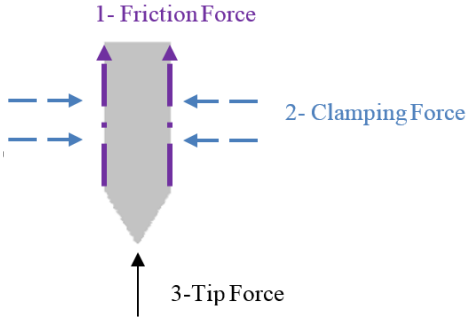

Fig. 5. Forces affecting the electrode.

illustrated in Figure 4c.

B. Electrode Mechanical Analysis

During insertion, the electrode inside the neural tissues experiences three mechanical forces [10]. During penetration, the tip force is the axial reaction acting on the electrode tip, and the clamping force is the normal force to the electrode surface. When the normal force acts on the surface, the coefficient of friction produces friction force along the electrode surface as illustrated in Figure 5.

The applied insertion force must be greater than the sum of these reaction forces in order to achieve successful penetration. Therefore, the insertion force was estimated to be 1mN [11].

The proposed designs are developed to provide axial stiffness to survive the mechanical forces experienced during insertion. The designs allow successful tissue penetration without the need for implantation stylus or similar stiffening devices.

There are two mechanical failure modes the electrode is subjected to on insertion: buckling and fracture. Accordingly, the Mechanical Analysis includes the studying of linear buckling, and stationary analysis with axial and shear loading. The conducted tests were done with different designs and several materials, each having its own failure mode based on its mechanical properties. The safety factor was calculated for each one of these tests for both ductile and brittle materials. Ductile materials such as Polyimide and metals (Cu and Ni) and brittle materials such as Silicon were used as materials for the implemented electrodes.

C. Linear Buckling Analysis

Buckling is a failure mode that takes place when the applied axial force exceeds the critical load [12]. The critical load value varies depending on the implemented electrode design and the material used. Thus, in order to avoid buckling failure, the electrode should be designed to have critical load higher than the force required for tissue penetration.

At the same time, to have high resistance to buckling failure, the electrode structure should be symmetric since buckling resistance diminishes with the existence of geometrical asymmetry, material defects, and eccentric loading [13].

Linear Buckling Analysis was applied on the electrode structures with different materials, while constraining the motion of the tip in all directions, thus creating fixed-free loading condition. A uniaxial unity force was applied to the electrode base. Buckling safety factor was calculated based on equation 1:

$$Safety\ Factor = \frac{failure\ load}{design\ load} \tag{1}$$

Where: the Failure load is the Critical load

Design load: Penetration force estimated to be 1mN [14].

D. Fracture Analysis

Stationary Analysis is applied to the electrode structure. Axial force was applied one time during axial stress and buckling failure analysis, while shear force was applied another time to the electrode base during shear stress analysis. The tip was fixed in its position using fixed constraint (fixed-free loading condition). A magnitude of 1N for axial force and 1mN for shear force was applied to the electrode base.

For analyzing axial stress acting on the electrode, the yield strengths for the used materials were used as indicated [15]. From the stress vs strain deformation diagram, the structure undergoes elastic deformation until it reaches the yield point, after which, it suffers plastic deformation till fracture. The von mises stress measured by COMSOL demonstrates the magnitude of stress levels. Von Mises stress or Equivalent tensile stress (σ_v) is a scaler form of von Mises yield criterion, calculated from the Cauchy stress tensor. It is used to predict the materials yielding when their maximum stress equals the maximum deformation stress that can be achieved experimentally in a tension test at yielding. The regions with maximum applied stress are used in safety factor calculations. These maximum stress points represent the regions where electrode failure starts. Equation 2 was used for calculating the safety factor for Axial Stress:

$$Safety\ Factor = \frac{Yield\ Strength\ Sy}{Von\ Misses\ Stress} \tag{2}$$

As for shear stress analysis, the maximum shear strength was obtained for each material. The maximum shear strength for ductile materials is half the ultimate tensile strength. On the other hand, the maximum shear strength for brittle materials is equal to the ultimate tensile strength (UTS). The maximum shear stress is calculated by Von Misses Stress or Tresca from COMSOL Multiphysics [14]. Tresca criterion states that yielding occurs when the difference between the maximum and minimum principal stresses is equivalent to twice the maximum shear stress that can be obtained experimentally in a tension test at yielding.

Both methods acquire almost the same results. Accordingly, equation 3 is used to calculate shear stress safety factor.

$$Safety\ Factor = \frac{Maximum\ Shear\ Strength}{Maximum\ Shear\ Stress} \quad (3)$$

III. Fabrication Process and Costs

The manufacture steps and expenses have been evaluated for every material. It ought to be realized that a few stages may require assist advancement so as to get the anode legitimately with its required structure. The principle manufacture steps actualized with Copper, Cu, and Nickel, Ni, are as per the following:

The first step is RCA-1 Si Wafer Cleaning. Then followed by Sputtering of thin layer of metal (Cu, Ni). The third step is deposition of Photoresist with thickness more than $100\,\mu m$ by Lithography and Spin Coating. Then making Cu Electroplating. After that an improvement of the surface roughness are performed by Chemical Mechanical Polishing CMP. Repeating the cleaning step and removing Photoresist by RCA-1. The last step is making the structure bio-compatible by using Gold Plating, since Ni and Cu are poisonous materials. The curvatures of the Ni may be encountered during the structure release where it is a high stress material.

For Si electrodes, SOI wafers will be used instead of Si wafers for Si material so the sputtering step will not be needed. The fabrication steps are:

RCA-1 SOI Wafer Cleaning. Followed by Lithography and Spin-coating of Photoresist to make a Photoresist layer. Then Deep Reactive Ion Etching (DRIE) of the wafer. After that, needing to repeat RCA-1 SOI Wafer Cleaning. And then use Dicing of the SOI wafers to get individual electrodes. KOH is used to make back side etching of the Si handle wafer to release the structure. And, finally removing oxide layer in the SOI wafer by HF.

Simpler steps are needed for the Polyimide material. The fundamental step is lithography to achieve the required thickness and using the appropriate developer.

1) Fabrication costs: The key factor affecting the expenses of designing any of the proposed electrode designs is the material used. Following the fabrication steps mentioned and using Si as the material will cost around $2100. However, using Cu and Ni will nearly cost the same amount of charges $1800, adding to this, the expenses of gold plating.

As for the Polyimide material, the material itself will cost almost $900, in addition to its required developer.

IV. Results

A. Linear Buckling

The simulation was run and swept for all materials for linear buckling analysis. The critical load factor outputs were used in safety factor calculations as in equation 1. The results are presented in Table I.

The buckling analysis results clearly favor designs E and C. The shorter base width in design A, B and D acted to its disadvantage. While, the circular junction design of F did not help it either. The simple designs with wide bases clearly triumphed with design E coming on top.

TABLE I. Liner buckling safety factor results.

Design	Materials	A,B	C	D	E	F
Single Stage	Si	30.6	35.7	32.9	36.7	33.4
	Cu	21.0	25.2	23.2	25.9	23.6
	Ni	41.9	46.0	42.4	47.3	43
	Poly	0.59	0.65	0.6	0.67	0.61
Two stages	Si	33.5	40.1	37.2	40.9	37.5
	Cu	21.7	28.3	26.3	28.9	26.5
	Ni	43.2	51.6	47.9	52.7	48.3
	Poly	0.61	0.73	0.68	0.75	0.68
Three stages	Si	38.7	46	43.1	47.1	43.1
	Cu	25.1	32.49	30.44	33.2	30.4
	Ni	49.8	59.27	55.55	60.6	55.5
	Poly	0.71	0.84	0.79	0.86	0.79

TABLE II. Axial stress safety factor results.

Design	Materials	A,B	C	D	E	F
Single Stage	Si	71.5	76.8	4.11	67.7	71.9
	Cu	0.7	0.78	0.04	0.69	0.76
	Ni	4.87	5.38	0.29	4.64	5.06
	Poly	0.4	0.44	0.02	0.41	0.46
Two stages	Si	62.5	55.1	3.83	51.4	51
	Cu	0.63	0.55	0.04	0.52	0.5
	Ni	4.29	3.78	0.27	3.53	3.48
	Poly	0.36	0.32	0.02	0.3	0.28
Three stages	Si	62.9	52.7	3.77	56.8	53
	Cu	0.63	0.53	0.04	0.57	0.53
	Ni	4.3	3.6	0.26	3.9	3.6
	Poly	0.36	0.3	0.02	0.33	0.31

Material wise, all designs satisfied the requirements of safety factor of 5 minimum except Polyimide. Ni was the top material of choice for buckling resistance. On the other hand, Polyimide had very weak mechanical properties that makes it unsuitable at this thickness. Increasing the thickness for Polyimide electrodes would make the device thicker than allowed for neural electrodes usage.

As predicted, increasing the number of stages of the shaft improved its buckling resistance. From single stage to two stages, nearly all electrodes gained around 10%-12% increase in safety factor. Another 14-16% increase was also noted on adding a third stage. This result was expected as a thicker shaft means more buckling resistance.

B. Axial Stress Analysis

Axial stress analysis was run under axial loading force of 1N. The results were analyzed and safety factor calculations were done as in equation 2. A minimum safety factor of 5 is required for a potential device as stated earlier. The results are tabulated in Table II.

Design D has significantly low values, this means that asymmetrical designs are poor choice and are susceptible to break easily. Design C was the best at single stage design but deteriorated faster at high stage counts. Significant changes in safety factor can be observed between single stages and two stages. The introduction of fillets between stages allows for the development of high stress values which can be blamed for this drop. Material wise, Silicon was had the best performance against axial stress loading and was the only material to satisfy

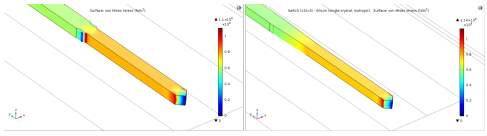

Fig. 6. The maximum stress in different designs, (**Left**) Design E with Fillet smoothing stage and its stress. (**Right**) Design E with Bezier polygon smoothing stage and its stress which is less than the stress in the left figure.

TABLE III. DESIGN E WITH BEZIER POLYGONS.

Design E 3 stages	Materials	Buckling SF	Axial Stress SF	Shear Stress SF
Equal lengths	Si	41.2	65.5	0.56
	Cu	29.1	0.69	1.9
	Ni	53.1	4.6	5.5
	Poly	0.75	0.41	0.5
Long Last Stage	Si	38.1	65.6	0.53
	Cu	26.9	0.69	1.9
	Ni	49.1	4.7	5.5
	Polyimide	0.7	0.41	0.5
Long First Stage	Si	46.3	61.6	0.55
	Cu	32.7	0.64	1.8
	Ni	59.7	4.3	5.3
	Poly	0.85	0.38	0.47

the minimum condition of 5 safety in all results. Polyimide and Copper performed very poorly in this analysis.

Design E had the best results in linear buckling analysis. In axial stress analysis, although it came only second to last in single stage design, the three stages design was able to compete better. A workaround for the issue caused with the introduction of fillets would improve these results. The designs using fillets versus Bezier polygons were compared next. Using design E for comparison, a stress plot in Figure 6:Left shows that the sharp stages causing a large stress and Figure 6:Right illustrates that the smoothing stages have a small stress .

Table III shows the results for buckling and axial stress analysis for design E with some modifications. As expected, axial stress safety was almost restored to the initial value of the single stage design. The results also compare modification of stage lengths. Axial stress safety did not suffer significant changes, but on the other hand, buckling safety change more considerably. The changes to buckling safety are expected, since decreasing the length of the wider stage means a thinner device overall which is more prone to buckling. These results show the tradeoffs between buckling resistance and total area. Both stage numbers and stage lengths can be tuned to achieve suitable design parameters.

C. Shear Stress Analysis

Shear loading analysis was run under a tangential boundary force of 1 mN. The results were computed and the maximum stress values were used in safety factor calculations in accordance with equation 3.

Table IV summarizes the results for shear stress safety factors. Asymmetry has failed design D in this test as well. Variations with number of stages does not follow a pattern. Design E had very small variations while design A, B and C had more significant drops. Design E had the best results among three stages designs, while designs A, B and C were

TABLE IV. SHEAR STRESS SAFETY FACTOR RESULTS.

Design	Materials	A,B	C	D	E	F
Single Stage	Si	0.65	0.64	0.34	0.56	0.58
	Cu	2.04	2.01	1.12	1.92	1.9
	Ni	6.06	6.03	3.3	5.52	5.6
	Poly	0.51	0.5	0.28	0.5	0.49
Two stages	Si	0.59	0.66	0.31	0.56	0.59
	Cu	1.87	2.05	1.01	1.92	1.86
	Ni	5.59	6.2	2.99	5.49	5.56
	Poly	0.47	0.5	0.25	0.49	0.47
Three stages	Si	0.51	0.5	0.34	0.55	0.47
	Cu	1.03	1.58	1.12	1.89	1.5
	Ni	4.85	4.73	3.3	5.44	4.49
	Poly	0.41	0.4	0.28	0.47	0.38

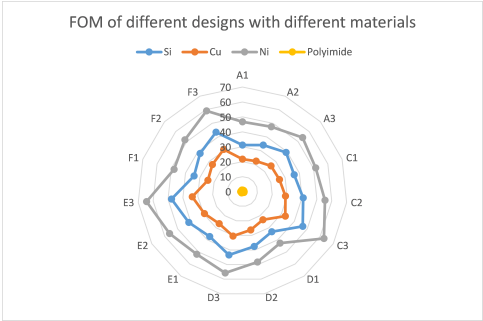

Fig. 7. The FOM for several designs with different materials (E1 is the shaft with only one stage, E2 is the shaft with 2 stages, E3 is the shaft with 3 stages).

better in single stage designs. The shear stress results for modified E designs are included in Table III. Material wise, Ni was by far the best. It is the only material that satisfied the minimum requirements of 5 safety factor.

D. Figure of Merit

In this part, a comparison between all designs was carried out to indicate which design is better. The comparison depends on the values of FOM. The best design has the largest value of FOM [6]. The FOM depends on the different values of safety factor for each design that were calculated from mechanical analysis as well as the fabrication cost of each material. All the other characteristics are constant for all designs such as impedance, noise, number of channels, and cross section area of the electrodes tip because of the pads all electrodes in these designs are constant.

Figure 7 illustrates the results of FOM. It shows that the design E with 3 stages with Ni material gives the highest value of FOM, so it is considered the best design. Design D with single stage and Polyimide material is considered the worst design because it gives the worst FOM.

V. CONCLUSION

Several electrode structures were introduced and analyzed to meet the design requirements using different materials.

The mechanical analysis results and fabrication cost estimation provide guidelines for the electrode design and material choice. The different designs ideas introduced several degrees of freedom in electrode design. Number of stages, stage length,

stage width as well as device material can all be tuned to achieve different mechanical performance.

It was clear that Ni possessed the highest buckling resistance during insertion followed by Silicon. Silicon had the best performance against axial stress loading. However, Polyimide and Cu performed very poorly in this analysis. As for shear analysis, results were in favor of Ni electrodes. Polyimide had very weak mechanical properties that makes it unsuitable at this thickness and at the same time using thicker Polyimide electrodes would make the device inapplicable for neural electrodes usage.

Asymmetrical designs are prone to breakage easily during axial stresses. Also, increasing the number of stages had an eminent effect on linear buckling resistance. Design E with three stages using Ni displayed capable mechanical performance and its FOM is the highest one. So depending on FOM values the best design is design E with 3 stages with Ni material and the worst one is design D with single stage and Polyimide material.

REFERENCES

[1] A. C. Hoogerwerf and K. D. Wise, "A three-dimensional microelectrode array for chronic neural recording," *IEEE Transactions on Biomedical Engineering*, vol. 41, no. 12, pp. 1136–1146, 1994.

[2] W. He and R. V. Bellamkonda, "A molecular perspective on understanding and modulating the performance of chronic central nervous system (cns) recording electrodes," 2008.

[3] B. Ghane-Motlagh and M. Sawan, "A review of microelectrode array technologies: design and implementation challenges," in *Advances in Biomedical Engineering (ICABME), 2013 2nd International Conference on*, pp. 38–41, IEEE, 2013.

[4] D. Kil, P. De Vloo, B. Nuttin, and R. Puers, "A foldable neural electrode for 3d stimulation of deep brain cavities," *Procedia Engineering*, vol. 168, pp. 137–142, 2016.

[5] H.-Y. Lai, L.-D. Liao, C.-T. Lin, J.-H. Hsu, X. He, Y.-Y. Chen, J.-Y. Chang, H.-F. Chen, S. Tsang, and Y.-Y. I. Shih, "Design, simulation and experimental validation of a novel flexible neural probe for deep brain stimulation and multichannel recording," *Journal of neural engineering*, vol. 9, no. 3, p. 036001, 2012.

[6] F. Kölbl and A. Demosthenous, "A figure of merit for neural electrical stimulation circuits," in *2015 37th Annual International Conference of the IEEE Engineering in Medicine and Biology Society (EMBC)*, pp. 2075–2078, IEEE, 2015.

[7] H. Draz, S. Gabran, M. Basha, H. Mostafa, M. F. Abu-Elyazeed, and A. Zaki, "Comparative mechanical analysis of deep brain stimulation electrodes," *Biomedical engineering online*, vol. 17, no. 1, pp. 1–14, 2018.

[8] S. R. Gabran, "Intra-cortical microelectrode arrays for neuro-interfacing," 2012.

[9] C. Multiphysics, "Introduction to comsol multiphysics®," *COMSOL Multiphysics, Burlington, MA, accessed Feb*, vol. 9, p. 2018, 1998.

[10] K. J. Paralikar, J. K. Lawrence, and R. S. Clement, "Collagenase-aided insertion of intracortical microelectrode arrays: evaluation of insertion force and chronic recording performance," in *2006 International Conference of the IEEE Engineering in Medicine and Biology Society*, pp. 2958–2961, IEEE, 2006.

[11] D. J. DiLorenzo and J. D. Bronzino, *Neuroengineering*. Boca Raton,FL: CRC Press, 2007.

[12] H. Kim and J. S. Colton, "Fabrication and analysis of plastic hypodermic needles," *Journal of medical engineering & technology*, vol. 29, no. 4, pp. 181–186, 2005.

[13] S. Gabran, M. T. Salam, J. Dian, Y. El-Hayek, J. P. Velazquez, R. Genov, P. L. Carlen, M. Salama, and R. R. Mansour, "3-d flexible nano-textured high-density microelectrode arrays for high-performance neuro-monitoring and neuro-stimulation," *IEEE Transactions on Neural Systems and Rehabilitation Engineering*, vol. 22, no. 5, pp. 1072–1082, 2014.

[14] M. Salcman and M. J. Bak, "A new chronic recording intracortical microelectrode," *Medical and biological engineering*, vol. 14, no. 1, pp. 42–50, 1976.

[15] S. D. Senturia, *Microsystem design*. Springer Science & Business Media, 2007.